Dyes and Pigments 5 (1984) 83–108

Azo–Hydrazone Tautomerism in Azo Dyes. IV. Colour and Tautomeric Structure of Adsorbed 1-Phenylazo-2-naphthylamine and 1-Phenylazo-2-naphthol Dyes

J. Kelemen

Research and Development Department, Dyestuffs and Chemicals Division

and

S. Moss and S. Glitsch

Central Function Research, Physics Department,
Ciga-Geigy Ltd, Basle, Switzerland

(Received: 12 November, 1982)

SUMMARY

The tautomeric compositions of 1-phenylazo-2-naphthylamines (**1**), *-naphthols* (**2**) *and their monosulphonates* (**3** *and* **4**) *have been investigated in the adsorbed state either on dyed polyester and wool fibres or in KBr pellets by means of scattered transmission, diffuse reflectance and Raman spectroscopy. The azo structure predominates in the naphthylamine series* (**1** *and* **3**) *in accord with previous results in solutions or with predictions by the perturbational molecular orbital theory. The major tautomer of the investigated naphthols* (**2** *and* **4**) *is mainly* **h**, *but both forms are present in* **2**(*p-MeO*) *and* **4**(*p-MeO*) *in comparable concentrations. Their* **h** *content depends on the nature of the substrate and increases in the order PES < WO < KBr. The colour is influenced by crystal field effects in the solid state as was shown for* **1**(p-NO_2). *Utilizing a set of inductively active substituents for R, the frequency of the first absorption band of the dyes correlates well with Hammett* σ, *yielding a positive slope with the hydrazones and a negative one with the azo tautomers. This behaviour leads to an inversion of the colour sequence upon changing the tautomer composition both in solution and in the adsorbed state and can be generalized by perturbational MO arguments.*

Dyes and Pigments 0143-7208/84/$03·00

1. INTRODUCTION

Hückel molecular orbital calculations[1] suggested great differences in the tautomeric behaviour of phenylazonaphthalene dyes (e.g. **1** and **2**), revealing strong dependencies on the nature of the protic donor substituent XH. Both tautomers are close in energy in the phenylazonaphthols, **2**, but in the naphthylamines, **1**, the azo form is favoured, as was proved recently both in solution[1,2] and in the crystalline state.[3]

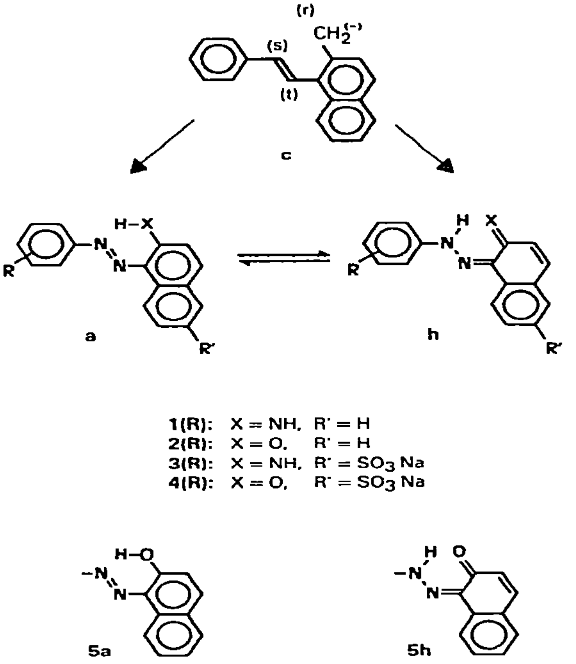

Scheme 1

These results can be generalized using Dewar's Perturbational Molecular Orbital (PMO) theory.[4] Accordingly, the tautomeric forms **a** or **h** of both series **1** and **2** can be derived from their common iso-π-electronic carbanion **c** by suitable replacements at sites r, s and t. The accompanying monoconcentric first-order perturbational energy contributions sum up to the following expressions:

$$E_a = E_c + (q_r - 2)\delta\alpha_{\ddot{X}} + (q_s - 1)\delta\alpha_{\dot{N}} + (q_t - 1)\delta\alpha_{\dot{N}} \quad (1)$$

$$E_h = E_c + (q_r - 1)\delta\alpha_{\dot{X}} + (q_s - 2)\delta\alpha_{\ddot{N}} + (q_t - 1)\delta\alpha_{\dot{N}} \quad (2)$$

where E is the π-bonding energy (E is negative for a bonded situation and differs in sign from $E_{\pi b}$, defined with thermochemical sign conventions in mind in Part I[1]) of one of the structures **a**, **h** or **c**, q is the charge density in the carbanion **c** which is particularly easy to calculate 'on the back of an envelope'[5] by the method of Longuet-Higgins[6] if **c** is odd and alternatant. The perturbation originating from the heteroatom is denoted by $\delta\alpha$ and the dots above the heteroatom symbols X and N give the numbers of electrons these atoms contribute to the π-system. Using the same Hückel parameters as in Part I, the energy difference to the tautomers, $\Delta E = E_h - E_a$, is then obtained for the two most interesting cases differing in X, namely

$$\Delta E = (q_s - q_r)\beta \qquad \text{for X} = \text{NH} \tag{3}$$

$$\Delta E = (q_s - q_r + \tfrac{1}{2})\beta \qquad \text{for X} = \text{O} \tag{4}$$

There will be no first-order contribution by the aza substitution at site **t**. The resonance integral β is negative *per definitionem* and, therefore, the hydrazone form, e.g. in **2** (X = O) is relatively more stable than in **1** (X = NH), the difference being $\beta/2$ (as follows from eqns (3) and (4)) or approximately 8–10 kcal/mol.

As no particular structural assumption had to be made for **c**, this treatment is quite general and eqns (3) and (4) can be applied to a great variety of compound classes involved in prototropic tautomerism, such as amino- and hydroxy-substituted *N*-heteroaromatics,[7] aromatic Schiff bases,[8] azo dyes[9] and others. In all these cases increasing electronegativity of the protic donor XH stabilizes the **h** type tautomer, whereas decreasing electronegativity shifts the equilibrium towards the **a** side. Consequently, in amino compounds the **a** form will be significantly more favoured than in the hydroxy analogues.

Taking the amply demonstrated fact of a mobile equilibrium, i.e. the temperature,[10–14] solvent[10,15,16] and substituent[10,16,17] dependence, as an indication of not too different tautomer energies in the naphthol dyes, **2**, the present results are fully compatible with the strong azo preference of the naphthylamines, **1**, investigated heretofore mostly in solutions.[1,2]

The aim of this paper is twofold: firstly, to establish the tautomeric composition of the title dyes under technologically relevant conditions *in the adsorbed state* on various substrates such as polyester (PES), wool (WO) or some inorganic standards using scattered transmittance, diffuse reflectance and Raman spectroscopic techniques, and secondly, to relate their colour to the equilibrium position in these systems.

The first attempt to obtain spectroscopic information on the tautomeric equilibrium of such dyes in the solid state was probably due to Hadži, who measured the scattered transmission of KBr pellets of three isomeric phenylazonaphthols in the visible region.[18] Generally, the sample is molecularly adsorbed on the diluent surface when organic solid materials are ground with inorganic standards.[19a] Therefore, Hadži's spectra refer to dyes in their adsorbed state. It was concluded, mainly from these measurements, that in **2(H)** both tautomeric forms are present in the solid state.[18] This apparently strange result has in the meantime been confirmed by X-ray work on some related dyes that showed that indeed both tautomers can participate in forming one and the same single crystal.[20] We shall present evidence in the course of this paper that in KBr discs at least great portions of the dye are in the amorphous state in which the presence of both tautomeric forms is, of course, not precluded.

Whereas the KBr pellet technique, applied in the visible spectral region, found little attention for tautomeric structure determination,[21] probably because of the poor quality of the early spectra, the measurement of diffuse reflectance of dyes seemed to be more popular.[22-25] The latter technique has been claimed to be of superior quality.[19b,22] Matsunaga *et al.* investigated the reflectance spectra of a number of substituted phenylazonaphthols, **2**, either diluted with sodium chloride[22] or deposited on filter paper,[23] polypropylene, polyacrylonitrile, polyester and nylon from acetone solutions.[24] Precipitation from an organic solvent, however, does not necessarily produce the same adsorbed state as application from an aqueous dyebath. Only few measurements have been published on properly dyed substrates such as nylon films[26] or nylon fabrics.[25]

2. EXPERIMENTAL

The dyes **1(R)**, **2(R)** with R = *p*-MeO, *p*-CN and *p*-NO_2, and **3(*p*-NO_2)** were the same as reported earlier.[1,2] The polyester fabrics were dyed during a period of 60 min at 130 °C to various depths of shade from a dyebath containing ammonium sulphate and a dispersant (Irgasol DAM) in suitable quantities. The dyed wool samples were kindly supplied by Dr H. Ackermann.

Raman spectra of KBr pellets and textile fabrics were recorded on a Cary Model 83 Raman spectrometer with a spectral bandwidth of

$\sim 10\,\mathrm{cm}^{-1}$ using a rotating sample holder to avoid excessive local heat evolution and thermal sample decomposition. Excitation at 488 nm ($\sim$40 mW at sample position) was with a Lexel Model 75 Ar^+ laser. Repeated scans showed excellent reproducibility. The KBr pellets contained approximately 1 mg dye in 700 mg KBr.

Thin layers (0·1–0·2 μm) of **1**(p-NO_2) were prepared in a Veeco VE 770-M evaporator at reduced pressure ($\sim 5 \times 10^{-6}$ Torr). The dye was heated not higher than 180 °C in a carbon crucible and the vacuum beam deposited on to a glass or quartz substrate held at ambient temperature at a distance of 80 mm.

Scattered transmission and diffuse reflectance spectra were recorded on a Beckman DK-2 and Beckman Acta M VI spectrometers, respectively. The Kubelka–Munk functions $F(R'_\infty) = K/S$ were calculated according to established formulae.[19c] The colorimetric calculations followed standard procedures.[27]

3. AZO-HYDRAZONE EQUILIBRIUM IN THE ADSORBED STATE

3.1. Results on dyed polyester fibres

The equilibrium position of dyes **1** and **2** has been established in a great variety of liquid solutions utilizing the solvent-induced spectral shift of their colour band in the electronic absorption spectra,[1] their Raman frequencies and NMR parameters.[2] Some of these data will be used for direct comparison with diffuse reflectance spectra of these dyes on PES, with scattered transmission spectra in KBr or with the Raman spectra both on PES and in KBr.

In Fig. 1 the normalized 1-chloronaphthalene (CLN) spectra of **1** and **2** are compared with their reflectance spectra obtained on PES. CLN was selected because its refractive index ($n_D = 1{\cdot}633$) is nearly coincident with that of PES ($n_D = 1{\cdot}53$ and $1{\cdot}73$, measured with light polarized parallel or perpendicular to the stretching direction of the fibre).[28]

Since the orientation relaxation time in polymeric substrates is generally expected to be much greater ($\geq 10^{-6}$ s) than the excited-state lifetime of the dye[29] (sub-nanosecond range for **2**(**H**)),[30] dispersion forces will dominate the solvent shift and, consequently, from the bulk solvent properties only the refractive index n will influence the band position to a

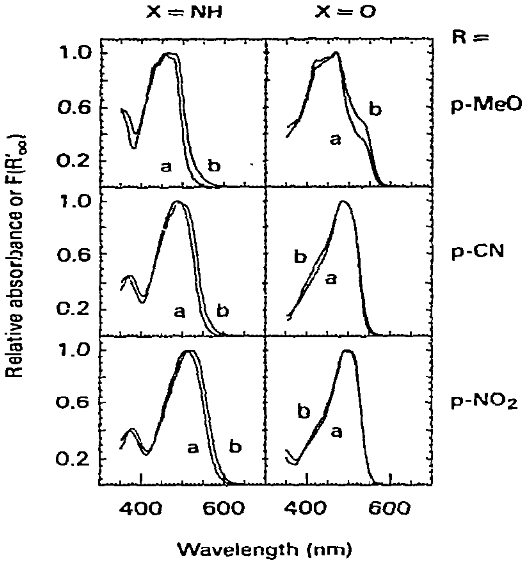

Fig. 1. Normalized absorption spectra of dyes **1**(R) and **2**(R) by measurements of (a) transmittance in 1-chloronaphthalene (10^{-5} M) and (b) diffuse reflectance on PES.

first approximation. In the absence of specific solvent effects, like H-bonding and CT-interaction, the band positions in CLN and on PES should therefore coincide, and thereby facilitate judgement of the tautomeric ratios.

The coincidence of band positions is nearly perfect with the naphthols. The comparison of **2**(*p*-CN) and **2**(*p*-NO_2) suggests identical tautomeric composition in either environment for both dyes. From the solution spectra an overwhelming hydrazone predominance has been claimed for these dyes in solvents of differing permittivities[1] and the same must be true for them in the adsorbed state on PES. For **2**(*p*-MeO) there is a slight increase in K_T observed by going from CLN to PES as judged qualitatively from the relative preponderance of the two absorption regions, 400–470 nm for the azo, and 470–550 nm for the hydrazone, form. This is, however, of the same magnitude as that found between the hydrocarbon solvent cyclohexane and all the other neat solvents investigated in Part I and is in accordance with the apolar character of polyester ($D = 3{\cdot}16$ to $3{\cdot}85$).[31]

The phenylazonaphthylamine spectra in Fig. 1 all show bands of very similar shapes both in CLN and on PES, the latter being red-shifted in the order of 10 nm, and are slightly broadened. We take these features as an indication of very close tautomeric ratios in both substrates, corresponding to azo predominance as was found in solutions,[1,2] and of a stronger intermolecular hydrogen bonding in PES which is responsible for the bathochromic shift and for the broadening. That the non-chelated NH_2-hydrogen of the naphthylamines is capable of H-bonding with oxygen functions of the surrounding molecules has been clearly demonstrated in 1(*p*-NO_2)-dioxane solvate by crystal structure determination.[3]

The Raman spectra of the dyed PES fabrics (Fig. 2) are in agreement

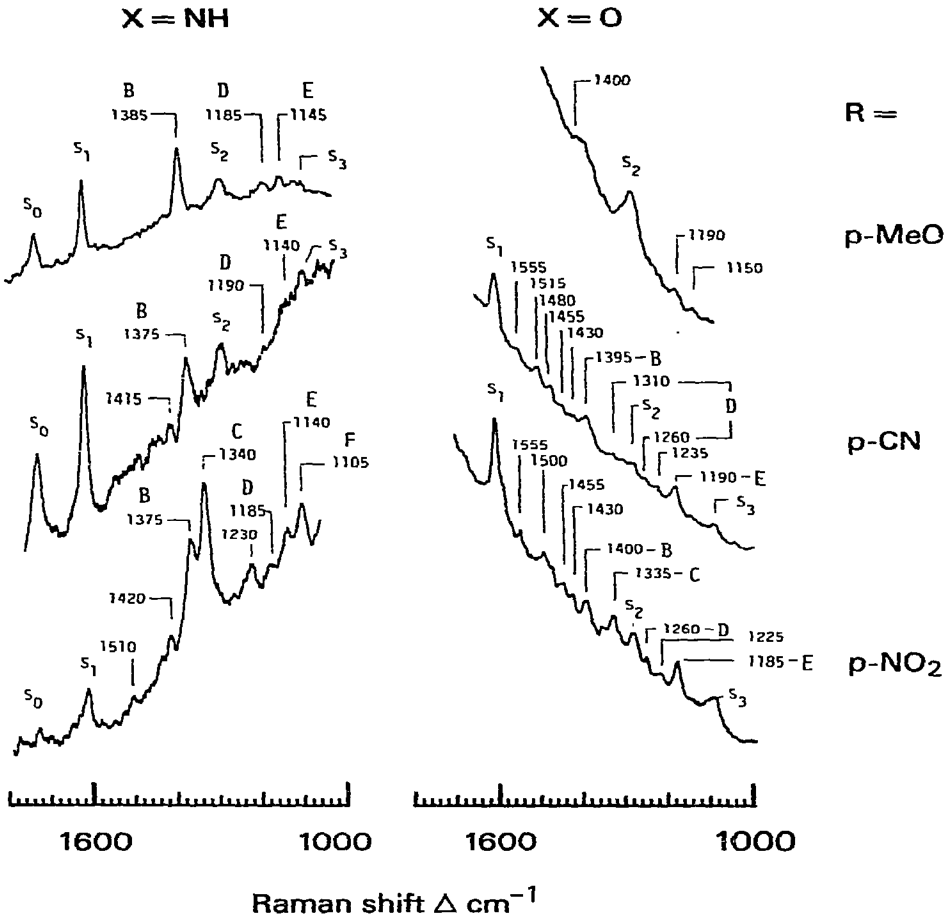

Fig. 2. Raman spectra of 1(R) and 2(R) on dyed PES substrate. For band assignment cf. Tables 1 and 2. The Raman lines of the substrate appear at 1730 (s_0), 1615 (s_1), 1290 (s_2) and 1095 (s_3) cm^{-1}.

with these conclusions. They exhibit besides the substrate lines s_0 to s_3 at 1730, 1615, 1290 and 1095 cm^{-1} the characteristic bands B and E near 1380 and 1140 cm^{-1} for the naphthylamines **1**. The latter have been assigned previously to the ν_1 and ν_2 modes in Lüttke's notation and correspond approximately to N=N and C—N stretching vibrations of the azo tautomer.[2] The skewed appearance of these spectra stems from the fluorescence emission of the substrate. Table 1 shows an excellent correlation with the carbon tetrachloride spectra, assigned to the azo form.[2]

The two naphthol derivatives with electron-withdrawing substituents, **2**(*p*-CN) and **2**(*p*-NO_2), exhibit a completely different intensity distribution as illustrated on the right hand side of Fig. 2. Both the correlation with frequencies obtained in CCl_4 (Table 2) and the oppositely tilted baseline are indicative of the hydrazone tautomer. Here the dye's own fluorescence overrides the emission from the PES support. Fluorescence,

TABLE 1
Raman Frequencies (cm^{-1}) Assigned to Azo Tautomers[a]

Assignment		*A* *Benzene* *(8a, 8b)*	*B* $\nu(N=N)$	*C* $\nu_s(NO_2)$	*D* $\delta(CH)+\nu(Ar—N)$	*E* $\nu(Ar—N)+\delta(CH)$	*F* $\nu(C—N)$ *nitro*
1(*p*-MeO)	CCl_4		1 387		1 183	1 444	
	PES	[b]	1 385		1 185	1 145	
	KBr	1 600	1 385		1 185	1 145	
1(*p*-CN)	CCl_4	1 600	1 374		1 185	1 142	
	PES	[b]	1 375		1 190	1 140	
	KBr	1 600	1 365		1 185	1 155, 1 135	
1(*p*-NO_2)	CCl_4	1 588	1 371	1 337	1 182	1 141	1 108
	PES	[b]	1 375	1 340	1 185	1 140	1 105
	KBr	1 590	1 370	1 330	1 180	1 140	1 105
2(*p*-MeO)	CCl_4[c]		1 400		1 180	1 145	
	PES	[b]	1 400		1 190	1 150	
	KBr		1 390		1 175	1 145	
3(*p*-NO_2)	H_2O	1 588	1 381	1 339	1 175	1 148	1 110
	WO	1 590	1 380	1 340		1 150	1 115
	KBr	1 590	1 385	1 335		1 145	1 110

[a] For solution spectra and assignment cf. ref. 2. Excitation wavelength: 488 nm except for solutions (514·5 nm).

[b] Obscured by PES signal.

[c] Excitation wavelength: 488 nm.

however, is not expected from the *trans*-azo forms on theoretical grounds and has not yet been observed.[32]

The Raman spectrum of **2**(*p*-MeO) is poor. The few barely recognizable lines at 1400, 1190 and 1150 cm^{-1} could be those of the azo structure, but again the strong baseline drift might arise from the other tautomer. The conclusion arrived at from the reflectance spectra, that both tautomers are present, is therefore probably correct, particularly if one considers the fact that the azo lines are generally more intense and the selective excitation of one compound only is always a possibility under resonance conditions.

3.2. Results on dyed wool fibres

The reflectance spectra of 18 phenylazonaphthol sulphonates **4**, substituted in any one of the *o*-, *m*- or *p*-positions of the phenyl ring, have been recorded on WO dyeings. Their Kubelka–Munk functions are plotted in Fig. 3 and the spectral data collected in Table 3.

The long wavelength absorption band of these dyes at about 500 nm corresponds undoubtedly to the **h** tautomer and the absorption region at around 420 nm to the **a** form in analogy to earlier assignments performed on unsulphonated derivatives **2** in solution.[16] Unfortunately, the exact

TABLE 2
Raman Frequencies (cm^{-1}) Assigned to Hydrazone Tautomers[a]

Assignment		*A* *Benzene* *(8a, 8b)*	*B* *Naphthalene ring*	*C* $\nu_s(NO_2)$	*D* $\nu(C—N)$ *Hydrazone*	*E* $\nu(N—N)$ *Hydrazone*	*F* $\nu(C—N)$ *Nitro*
2(*p*-CN)	CCl_4	1 610	1 395		1 308 1 294 1 260	1 182	
	PES	[b]	1 395		1 310 1 260	1 190	
2(*p*-NO_2)	CCl_4	1 599	1 401	1 342	1 299 1 261	1 188	1 114
	PES	[b]	1 400	1 335	1 260	1 185	[b]
	KBr	1 610	1 400	1 335	1 260	1 190	1 105

[a] For solution spectra and assignment cf. ref. 2. Excitation wavelength: 488 nm except for solutions (514·5 nm).

[b] Obscured by PES signal.

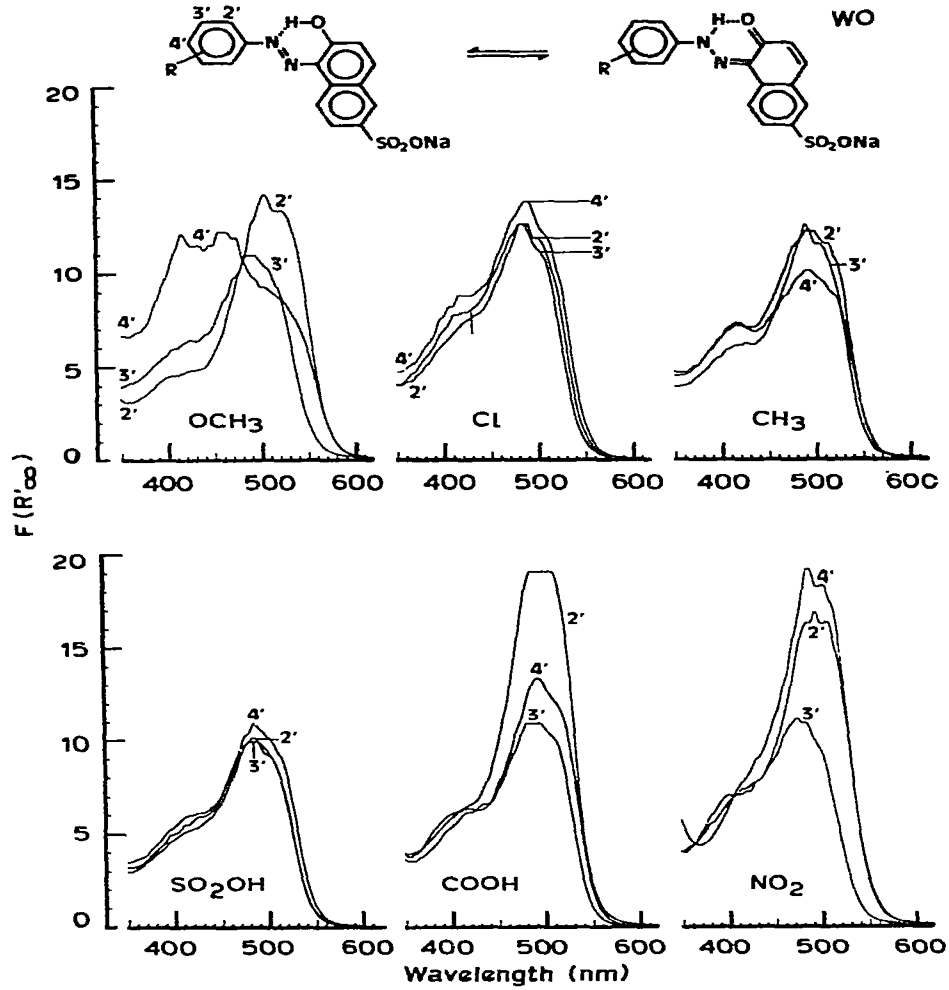

Fig. 3. Absorption spectra of 4(R) on dyed WO substrate from reflectance measurements.

value of K_T cannot be determined from the strongly overlapping spectra. The 'ratio $\varepsilon_h/\varepsilon_a$ of the molecular extinction coefficients at the maxima of the observed two bands (sometimes estimated from broad inflexions)' was used by Burawoy *et al.* as an approximate measure for the equilibrium position.[16] For the wool samples dyed with 4 the analogously taken ratio of the Kubelka–Munk functions serves the same purpose as the ratio of extinction coefficients in solution. These values are for all cases where

TABLE 3
Some Spectroscopic and Colorimetric Properties of Dyed Textile Materials[a]

No.	*Dye/Fibre*	λ_{max} *(nm)*	σ_R	λ_d *(nm)*	p_e	*Y*
h-*Transitions* (*Group I*)						
1	4(*p*-Me)/WO	493	−0·170	594·6	79·39	32·00
2	4(*m*-Me)/WO	493	−0·069	592·6	81·26	33·43
3	4(*m*-SO_3^-)/WO	485	0·05	588·7	81·3	40·01
4	4(*p*-SO_3^-)/WO	485	0·09	590·7	80·29	36·81
5	4(*m*-MeO)/WO	490	0·115	594·4	78·10	30·48
6	4(*p*-Cl)/WO	488	0·226	592·6	84·26	33·63
7	4(*m*-COOH)/WO	487	0·355	590·6	81·18	36·84
8	4(*m*-Cl)/WO	483	0·373	589·4	84·46	37·90
9	4(*m*-NO_2)/WO	475	0·710	586·8	83·87	40·47
10	4(*o*-Me)/WO	490		595·0	79·13	31·95
11	4(*o*-Cl)/WO	488		591·3	83·25	36·00
12	4(*o*-SO_3^-)/WO	485		588·8	80·02	39·15
h-*Transitions* (*Group II*)						
13	2(*p*-MeO)/PES	517[b]	−0·268	590·9	62·95	42·79
14	2(*p*-CN)/PES	488	0·628	587·1	67·02	49·41
15	2(*p*-NO_2)/PES	490	0·778	590·2	68·54	42·82
16	4(*p*-MeO)/WO	523[c]	−0·268	600·7	80·73	23·02
17	4(*p*-COOH)/WO	493	0·265	593·9	80·67	32·96
18	4(*p*-NO_2)/WO	488	0·778	594·6	83·52	28·35
19	4(*o*-MeO)/WO	505		608·5	67·92	21·38
20	4(*o*-COOH)/WO	498[d]		594·0	81·15	27·34
21	4(*o*-NO_2)/WO	495		595·9	81·90	28·70
a-*Transitions* (*Group I*)						
22	3(*m*-MeO)/WO	448	0·115	583·4	53·11	47·93
23	3(*m*-NO_2)/WO	478	0·710	586·0	64·79	40·27
a-*Transitions* (*Group II*)						
24	1(*p*-MeO)/PES	462	−0·268	580·9	57·37	58·76
25	1(*p*-CN)/PES	495	0·628	592·8	42·92	47·07
26	1(*p*-NO_2)/PES	520	0·778	−493·3[e]	32·81	25·67
27	3(*p*-MeO)/WO	454	−0·268	582·1	52·64	46·55
28	3(*p*-NO_2)/WO	510	0·778	619·8	42·40	18·51
29	3(*o*-MeO)|WO	450		584·1	53·75	48·70
30	3(*o*-NO_2)/WO	498		600·0	58·20	21·31

[a] λ_{max}, Wavelength of colour band maxima; σ_R, Hammett substituent constant;[49] λ_d, dominant wavelength;[27] p_e, excitation purity;[27] *Y*, brightness.[27]

[b] Estimated from the difference between PES and CLN spectra; λ_{max} of the a-transition: 468 nm.

[c] Estimated from the difference between WO and CLN spectra; λ_{max} of the a-transition: 457 nm.

[d] Midpoint of a truncated band (cf. Fig. 3).

[e] Complementary wavelength.[27]

common substituents R permit a comparison consistently higher at about 0·3 than those of Burawoy for the unsulphonated dyes **2** in ethanolic solution. The additional stabilization of the **h** tautomer in **4** does not result from the electronic effect of the SO_3^- group as quantum chemical calculations suggest a slight azo shift upon sulphonation.[1] Its origin should rather be sought in specific interactions either with the substrate or with other dye molecules forming dimers or higher aggregates.

The naphthylamine dyes **3** are in the azo form on wool. They absorb at nearly the same wavelengths as their unsulphonated analogues on PES. Thus, the positions of the maxima on both substrates are very similar as in the case of **3**(*p*-MeO) (PES, 463; WO, 455 nm) or **3**(*p*-NO_2) (PES, 517; WO, 515 nm). Furthermore, the Raman spectrum of **3**(*p*-NO_2) on wool compares favourably with other azo structures listed in Table 1. Acid strengthening groups R in *o*- and *p*-positions increase the phenylhydrazone concentration as was shown for the naphthol derivatives experimentally[16] and for both naphthols and naphthylamines by molecular orbital calculation theoretically.[1] Therefore, if the nitro dye **3**(*p*-NO_2) is entirely on the azo side as the Raman results suggest, substituents with weaker electron-withdrawing or -donating character will favour the azo form even more.

3.3. Results on inorganic substrates

By measuring the spectra of dyes **1** and **2** on inorganic standards, some complications emerged. These are described first. The transmittance spectra of KBr discs showed sometimes a new, more or less well resolved band in the long wavelength region. This was particularly striking in the case of **1**(*p*-NO_2) with a band positioned between 600 and 650 nm which is absent in both solution and polyester spectra. A pronounced Christiansen effect in the IR paralleled the appearance of the new band indicating some dependence on particle size. Figure 4A displays a few examples: KBr discs of **1**(*p*-NO_2), prepared at a constant dye concentration (0·04%) but with increasing grinding times, showed diminishing absorbance above 600 nm (curves a–c). Wetting the KBr–dye mixture with CH_2Cl_2 prior to grinding and pelleting enhances the effect of prolonged grinding (curve d). A similar behaviour is observed in the reflectance spectra of $BaSO_4$ preparations of the same dye. Chemisorption, such as has been reported, for example, with *p*-dimethylaminoazobenzene on extremely dry $BaSO_4$,[33] can be ruled out, for the

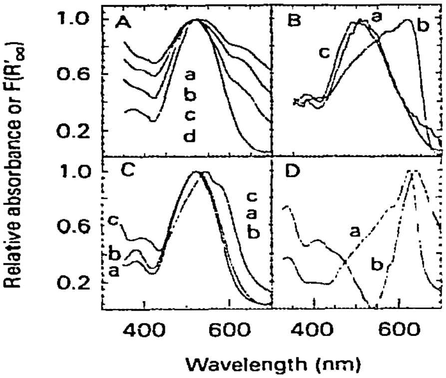

Fig. 4. Effect of sample preparation on the solid-state light absorption of 1(p-NO_2). The normalized spectra were obtained from measurements of: (A) Scattered transmittance of KBr discs ground prior to pelleting for (a) 60, (b) 120 and (c) 240 s at ~0·04% dye concentration without added CH_2Cl_2, and (d) ground for 90 s with added CH_2Cl_2 at 0·015%. (B) Diffuse reflectance of 0·1% dye in $BaSO_4$ (a) before and (b) after wetting with, and consecutive evaporation of, $CHCl_3$; (c), as (b), after removal of the surface layer. (C) Scattered transmittance of (a) KBr discs ground with added CH_2Cl_2 prior to pelleting; (b) vacuum deposited amorphous red film, and (c) violet polycrystalline film (see text). (D) Scattered transmittance of the blue polycrystalline film (a), and difference spectrum of KBr discs (b) described in text.

adsorbent was not meticulously dried in the present case and also because the new band disappeared with dilution.

If we assume that prolonged grinding produces increasing amounts of amorphous material at the expense of crystalline particles, then curves a to d in Fig. 4A differ mainly in the adsorbed-amorphous to crystalline ratio. Hence, the difference spectrum between any two of these curves should be characteristic of the-absorption in the crystalline state, whereas curve d itself corresponds to the adsorbed amorphous form. Curve b in Fig. 4D is such a difference spectrum, being renormalized after subtracting curve d from c in Fig. 4A.

Further evidence that spectral effects of this type and magnitude can originate from a crystalline-to-amorphous transition or *vice-versa* is seen in Fig. 4B. Curve a is the reflectance spectrum of 1(p-NO_2), ground with $BaSO_4$ at a 0·1% dye concentration. Thereafter, the sample was moistened with a few drops of chloroform and allowed to dry at room temperature. Its colour changed from red to blue and a thin polycrystalline film was formed through migration of the dissolved dye to the surface by capillary action and consecutive evaporation of the solvent.

The resulting spectrum of this sample is strongly red-shifted (curve b). After removing the top crystalline layer, curve c, which is very similar to the original spectrum (a) except in the region above 600 nm, is obtained. The long-wavelength toe, obviously of crystalline origin and clearly discernible in a, has now disappeared.

The evaporation of organic molecules under reduced pressure has been widely used as a method for producing polymorphic material.[34-39] Vacuum-deposited thin (~0·1–0·2 μm) films of **1**(p-NO_2) on glass or quartz plates were studied next. Immediately after vapour-phase quenching of the dye on to the cool substrate a compact amorphous coating was achieved. On standing at ambient temperature spontaneous crystallization started within 10–60 min, yielding either violet or blue polycrystalline films, or greater crystalline aggregates with disruption of the homogeneous layer. Exposure to water vapour or methylene chloride vapour accelerated the process and the blue film was formed exclusively. In Fig. 4C the scattered transmission spectra of the amorphous (curve b, $\lambda_{max} = 520$ nm) and of the violet film (curve c, $\lambda_{max} = 543$ nm) are shown and in Fig. 4D the spectrum of the blue layer is displayed (curve a, $\lambda_{max} = 625$ nm). Under the microscope, both the violet and the blue films showed red markings, originating from freshly produced amorphous material, when scratched with a sharp-edged tool.

Using differential scanning calorimetry at a heat transfer rate of 10 °C min^{-1} the original crystalline **1**(p-NO_2) material melted at 187·0 °C. This was the sole phase transition of this sample. On cooling the melt solidified at about 125 °C and a repeated scan with the same probe revealed a second polymorph, melting at 165·7 °C. After a subsequent exothermic transition at about 168–169 °C a final melting at 185·9 °C was recorded. The bulk amorphous material, obtained by scraping off the vacuum-deposited film from the glass support, showed a weak exothermic transition between 105 and 126 °C and a gradual melting around 156–160 °C. No further information was gained on the amorphous material as partial crystallization probably occurred during the transfer from the glass substrate to the calorimeter pan.

Referring to Fig. 4C, the absorption maximum of the KBr sample prepared with added methylene chloride (520 nm, curve a) is identical within the accuracy of the measurement to that of the amorphous red film (curve b) and compares favourably with values obtained either in dimethylformamide (517 nm)[1] or in polyester (520 nm). The amorphous nature, i.e. the random orientation, of the dye molecules in a thoroughly ground KBr pellet, particularly if prepared by adding a suitable organic solvent, is therefore established beyond doubt. The small variations in the wavelengths of the maxima are in a range typical of medium effects.

In Fig. 4D the transitions of the vacuum-deposited blue polycrystalline film (337, 390–420, 587 (s) and 625 nm, curve a) fit well with those of the difference spectrum (338, 405, 582 (s) and 640 nm, curve b). Some intensity distortions are inherent in the latter method. We assume, therefore, that these spectra approximate to the true spectrum of the bulk crystalline material (m.p. 187·0 °C) whereas the spectrum of the violet film (curve c in Fig. 4C) belongs to another polymorph, possibly the one revealed in the calorimetric experiment (m.p. 165·7 °C).

The strong red shift accompanying the amorphous-to-crystalline transition is believed to be brought about by crystal field (Davidov) splittings. Monahan *et al.* observed the same phenomenon among others in arylazonaphthol dyes such as **2**(H) or CI Pigment Red 31.[34,36] The bathochromic shift found in the latter case was explained as arising from resonance interactions of excited states of coupled aggregates, referring to the molecular exciton model advanced by McRae and Kasha.[40] Accordingly, a molecular arrangement in card-pack fashion with a slightly tilted array of molecules was concluded with tilt angles defined between the transition dipole of the molecule and the translational direction.

The observed bathochromic transition in the crystal spectra of **1**(*p*-NO_2) might have a similar origin and a parallel stacking of the dye molecules with small tilt angles in the crystal lattice is one of the possibilities. With the experimental evidence to hand, however, no detailed proposal regarding the packing scheme can be made.

After having ensured that the anomalous band is of crystalline origin, arising from incomplete homogenization of the sample and not related directly to the tautomeric problem, the wet grinding KBr pellet technique has been used to obtain scattered transmission spectra of the other dyes in their adsorbed amorphous state (Fig. 5).

The tautomeric composition can readily be understood from a comparison with CLN and PES spectra, shown in Fig. 1. As expected, the naphthylamines, **1**, which are stabilized far on the azo side of the equilibrium in any medium examined up to now, are exclusively in the azo form also if adsorbed on potassium bromide. Similarly, for the naphthols **2**(*p*-CN) and **2**(*p*-NO_2) the hydrazone predominance can be verified in this way.

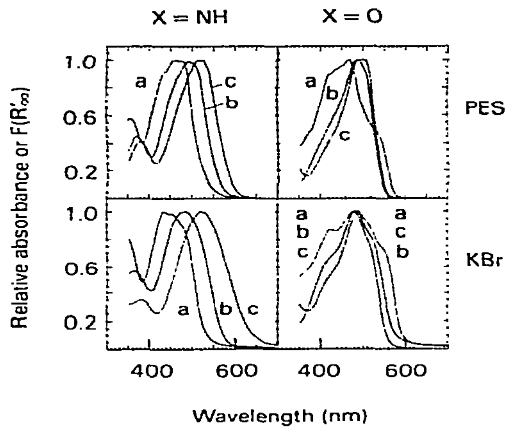

Fig. 5. Normalized diffuse reflectance (top) and scattered transmittance (bottom) spectra of **1**(R) and **2**(R) in dyed PES substrate or in KBr pellets. R = *p*-MeO (a), *p*-CN (b) and *p*-NO_2 (c).

The KBr spectrum of **2**(*p*-MeO), the sole compound in these series with a mobile equilibrium, indicates a strong hydrazonic shift as compared with the spectra in solutions or on polyester. The **h** tautomer is even more stabilized here than in **4**(*p*-MeO) on wool. The 499 nm transition of the hydrazone is the most intense in this case, but a shoulder at 435 nm shows also a sizeable concentration of the **a** form which gives rise to an azo-type Raman signature (*vide infra*).

The hydrazonic stabilization through adsorption on to ionic crystal lattices is not without precedence. The **h** tautomer is nearly the exclusive species when **2**(H) is adsorbed on 'highly polar' surfaces, e.g. on silica gel[34] or on sodium chloride.[41] The first layers of **2**(H) are deposited as the hydrazone tautomer on glass plates upon quenching from the vapour phase, but the consecutive ones are piled up in the azo form[42] showing great dependence on the nature of the adsorbing surface.

The Raman spectra in KBr are displayed in Fig. 6. They are better resolved than those in PES and no obstruction from the Raman and fluorescence emission of the substrate appears. The derivatives of **1** have the **a** structure and **2**(*p*-NO_2) is predominantly **h** as follows from the correlations in Tables 1 and 2. The persistent fluorescence of the naphthol dyes **2**, which prevented the recording of **2**(*p*-CN) and is manifested in the spectra of the two other derivatives by the strong baseline drift, is noteworthy.

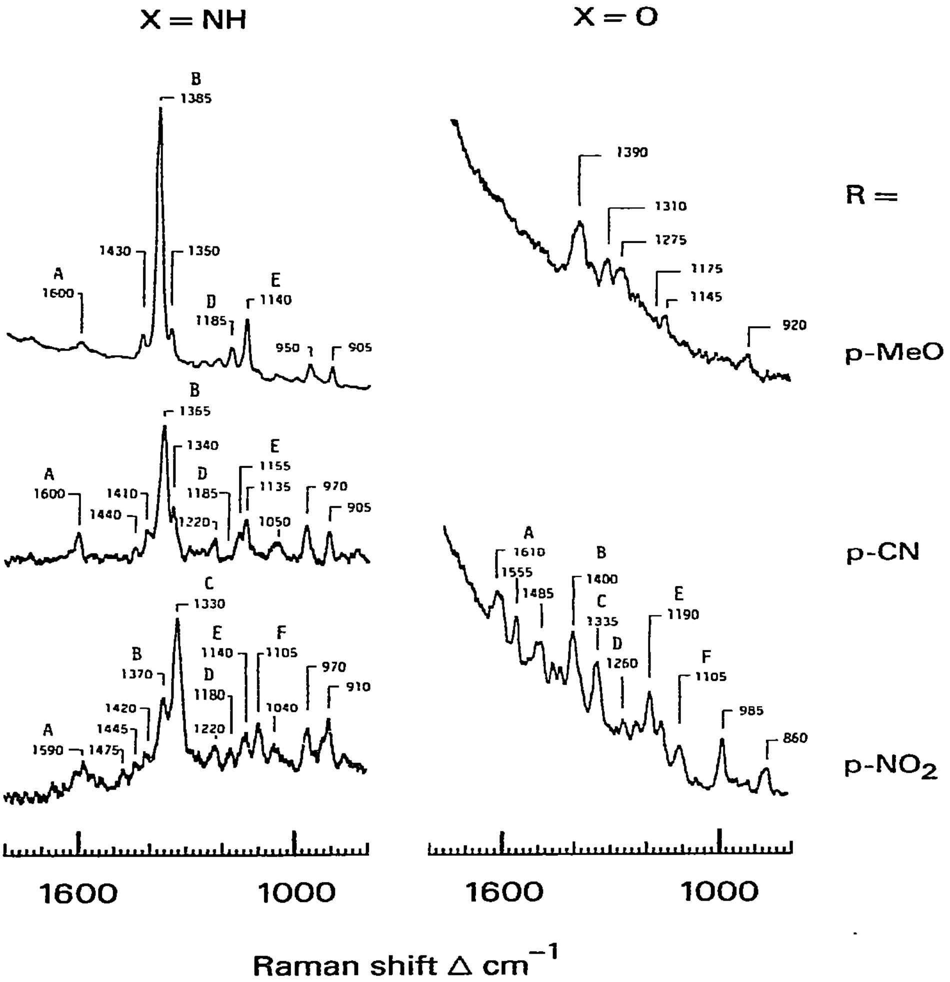

Fig. 6. Raman spectra of dyes **1** and **2** in KBr discs.

Previously, when using the 514·5 nm Ar$^+$ line for excitation, no solution spectrum of **2**(*p*-MeO) could be recorded due to fluorescence problems.[2] By exciting at 488 nm it is now possible to obtain a spectrum in carbon tetrachloride which is very similar to that in KBr. Its Raman frequencies, arising from the azo form, are included in Table 1. Based on Raman evidence alone neither **a** nor **h** can be rigorously excluded for **2**(*p*-MeO) in any of the investigated environments.

To summarise this section, a strong azo preference has been established for the 1-phenylazo-2-naphthylamine derivatives investigated (**1** and **3**) in the adsorbed state on polyester, wool and on some inorganic ionic crystal lattices. This contrasts with the behaviour of the analogous naphthol dyes (**2** and **4**), which are either predominantly in the hydrazone form on all substrates considered or have comparable tautomer energies (e.g. **2**(*p*-MeO)) judging from the mobility of the equilibrium.

The experimental evidence presented here and elsewhere[1-3] verifies fully the claim derived from perturbational theory according to which the azo form becomes substantially stabilized relative to the hydrazone tautomer if the protic donor XH changes from OH to NH_2. As a consequence, dramatic colour changes occur which will be discussed in the following section.

4. COLOUR PROPERTIES

Changing equilibrium position in a tautomeric dye has an influence on colour comparable with that of changing substituents in a single structure; moreover, one and the same substituent can yield differing colour shifts in the two tautomers, by both sign and magnitude. In the azo-type WO samples of **3**, for example, the powerful electron acceptor *p*-NO_2 produces a more red-shifted hue than does the electron-donating *p*-OMe group. The opposite behaviour is observed for the hydrazonic naphthol dyes **4**, where the MeO derivative is the more bathochromic. This is best illustrated by the chromaticity coordinates, displayed in Fig. 7. The same applies to the *o*- and, to a lesser degree, *m*-substituted dyes as shown in spectral terms in Fig. 8. From the spectra in Figs. 1 and 5, it is inferred that a similar relationship holds for the non-ionic **1** and **2** in PES, in CLN solutions and in inorganic substrates. Not only does the nature of the protic donor XH alter the tautomer composition, but as a consequence of the equilibrium shift an inversion of the colour (hue) sequence can result within a given set of R.

This phenomenon is not without precedence. In 4-phenylazo-1-naphthols[43] and in 4-phenylazo-2,6-di-*t*-butylphenols[44] a positive slope has been observed in solution for the **h** and a negative slope for the **a** tautomer when the frequency of the colour band maximum ($\bar{\nu}$), is plotted against σ_R, the Hammett substitution constant of R. The corresponding correlation coefficients were noted to be rather poor.[43,44]

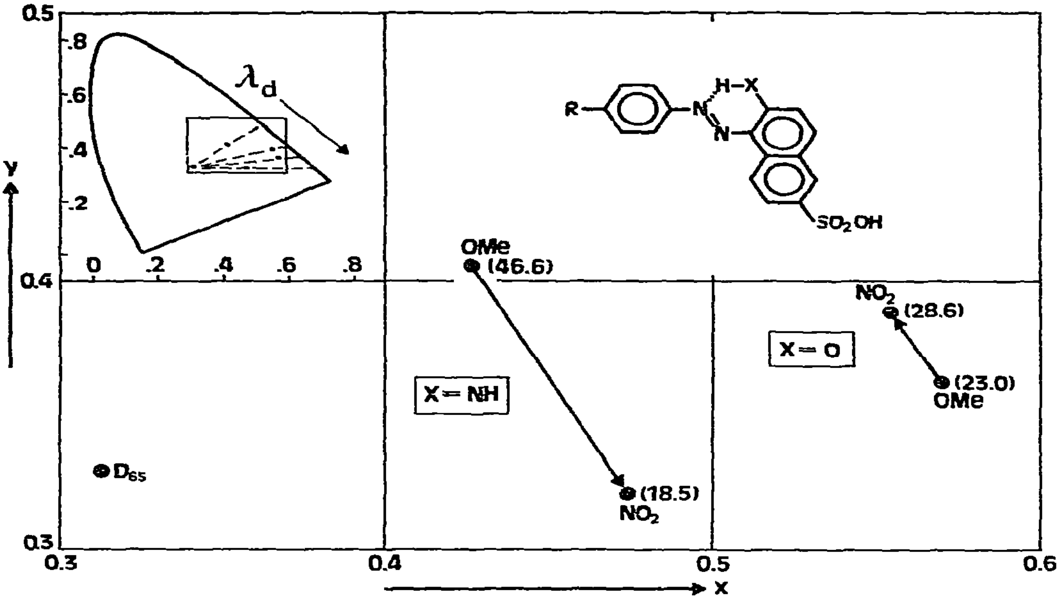

Fig. 7. Enlarged portion from the chromaticity diagram (insert, top left) showing inversion of the colour (hue) sequence in the naphthylamine (3) and naphthol (4) dye series on WO. The arrows point in the direction of increasing Hammett σ_R and the numbers in parentheses describe sample brightness Y. Sense of increasing dominant wavelength is indicated in the insert figure.

It can be shown by PMO theoretical arguments along the lines put forward by Gerson and Heilbronner[45] that a linear relationship between $\tilde{\nu}$ and σ_R with all types of substituents can only be expected if the electronic transition which gives rise to the considered absorption band is localized in a remote part of the molecule, not including the substitution site itself. If this condition is fulfilled, the conjugative effect which arises from the extension of the π-system by the substituent vanishes and the spectral shifts are governed by inductive effects only. The excellent linear correlation found for the first localized transition of 1-phenylazoazulenes proves this point.[45]

The presently investigated tautomeric structures do not comply with the above criterion. For these the first transition is delocalized over the entire chromogen as shown in Fig. 9 (a and c). Therefore, with certain substituents a sizeable conjugative contribution might arise which, representing second-order perturbations, depends on the MO population both in the parent dye and in the substituent at the attachment site as well

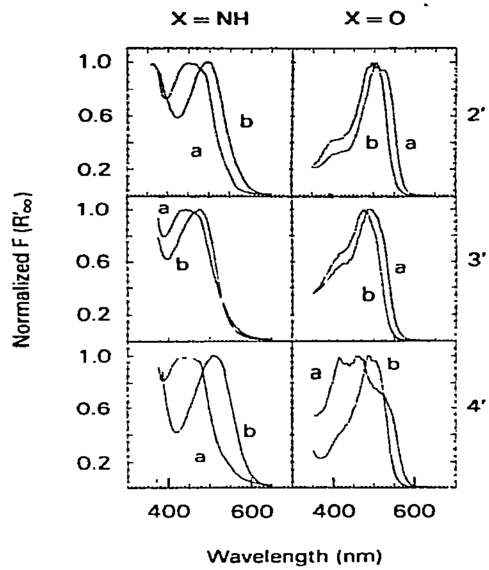

Fig. 8. Inversion of the colour band positions in the naphthylamine and naphthol dye series 3(R) and 4(R) with R = MeO (a) or NO_2 (b).

as on the relative energies of the interacting MOs. It results always in a bathochromic shift,[45] is unrelated to σ_R and can become detrimental to the linearity of the regression. We believe that this accounts at least for the major part of data-point scatter that leads to the above cited[43,44] and other reported[46-48] poor correlation coefficients in Hammett-type plots of absorption frequencies.

The correlation can be improved, however, by restricting the regression line to points with negligible conjugative interaction of the substituent. This can be achieved with all substituents in the *m*-position, where the MO coefficients are small both in HOMO and LUMO of the parent molecule (cf. Fig. 9, a and c) or with some selected *p*-substituents which lack strongly interacting substituent orbitals (e.g. CH_3, CF_3) or with substituents with energetically unfavoured AOs (F and possibly Cl).

The straight lines drawn in Fig. 10 are computed for such restricted sets of substituents (Group I). They represent **a**-transitions of **1** in methylcyclohexane solution from literature data[48] and **b**-transitions of **4** on WO from our own measurements, collected in Table 3. The empty symbols refer to substituents with non-negligible conjugative interaction (Group II). As expected, the latter are always bathochromically displaced

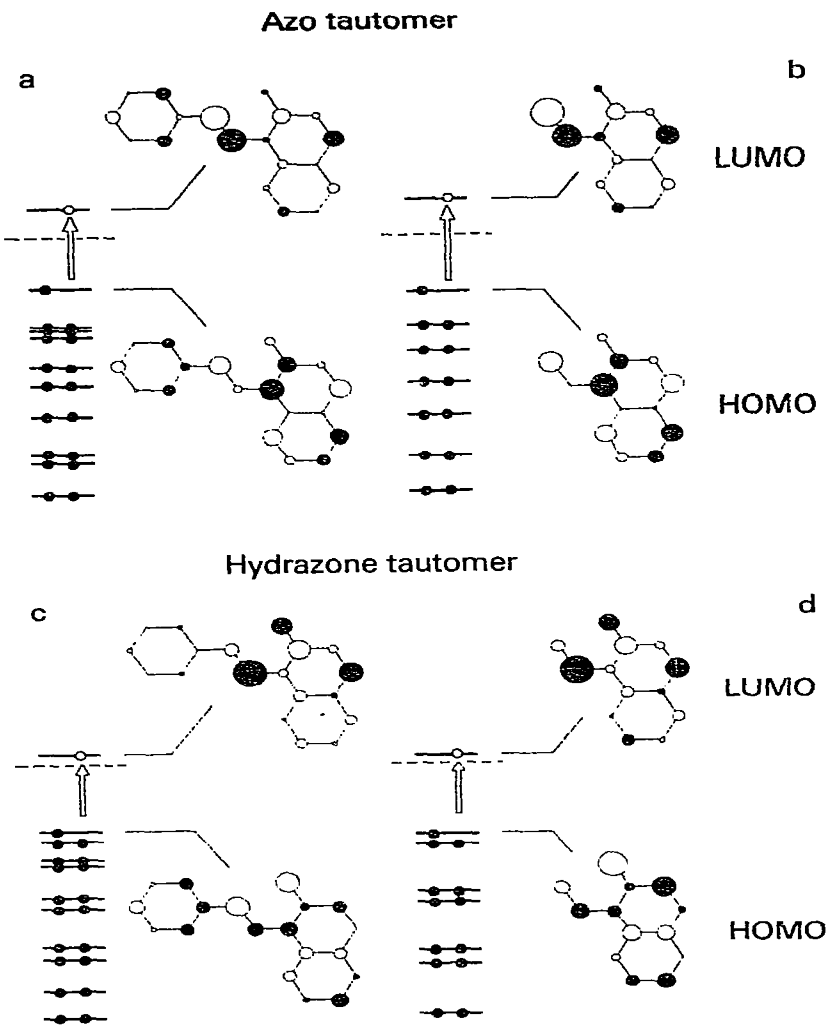

Fig. 9. Orbital energy schemes and pictorial representation of MOs involved in the first transition of (a) **2(H)-a**, (b) **5a**, (c) **2(H)-h** and (d) **5h**.

from the line, i.e. towards lower wavenumbers. For comparison the few PES data of **2h** are also included in Fig. 10b. Neither these nor the a-transition data on WO or PES are, however, numerous enough to warrant a regression analysis, but the λ_{max} and λ_d values in Table 3 are not in contradiction to the present approach.

The differing signs of the slopes in Fig. 10 obviously depend on the

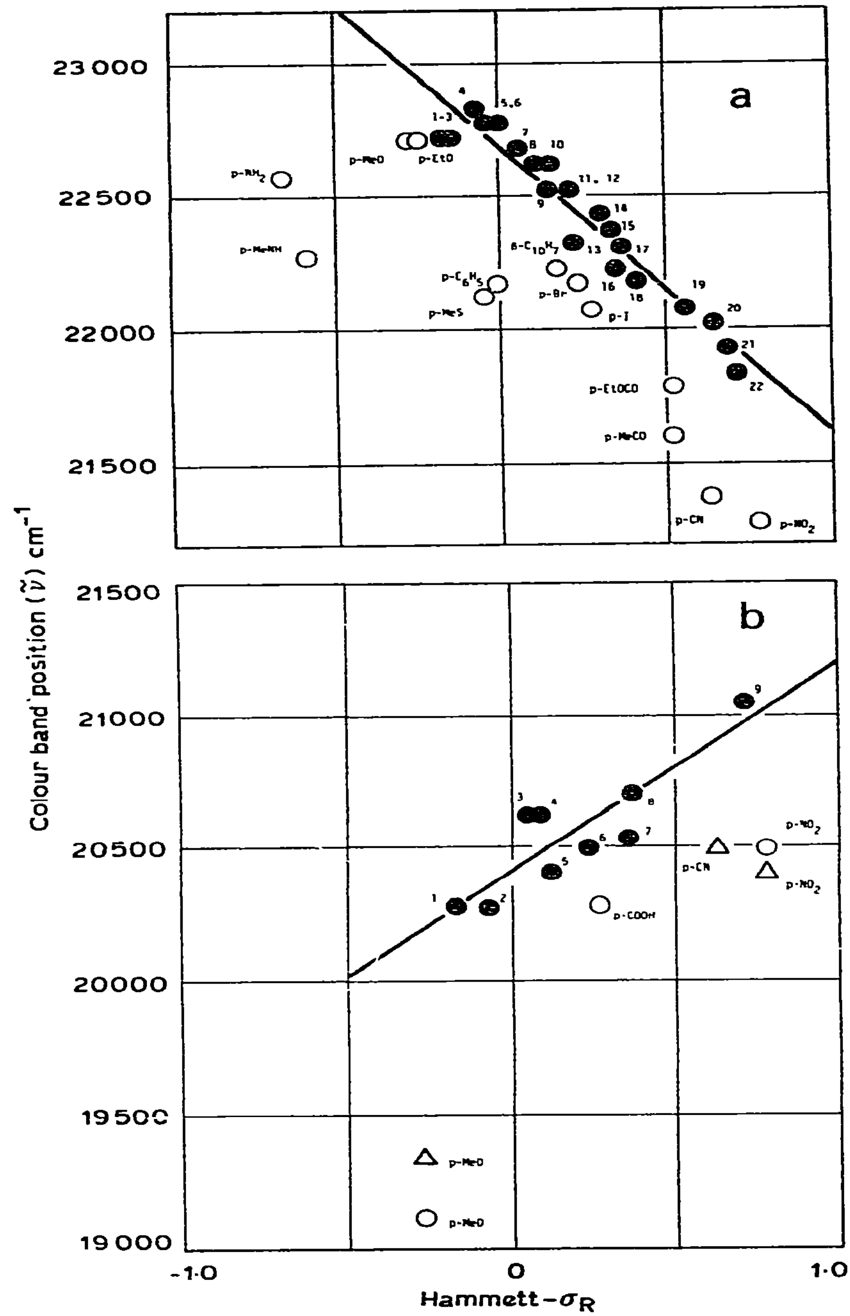

Fig. 10. Correlations of colour band position with Hammett σ_R. The regression lines are drawn for the numbered (black) points. R = *p*-Me (1), *m*-NH$_2$ (2), *p*-Et (3), *m*-Me (4), *m*-Et (5), H (6), *p*-F (7), *m*-MeO (8), *m*-MeS (9), *m*-EtO (10), *m*-AcNH (11), *m*-C$_6$H$_5$ (12), *p*-Cl (13), *m*-MeCO (14), *m*-F (15), *m*-I (16), *m*-Cl (17), *m*-CF$_3$ (18), *p*-CF$_3$ (19), *m*-MeSO$_2$ (20), *m*-CN (21), *m*-NO$_2$ (22). (a) Azo transitions of dyes **1(R)** in methylcyclohexane (MCH).[48] (b) Hydrazone transitions of dyes **2(R)** and **4(R)** measured on PES (△) and on WO (○, ●) substrates. Data from Table 3.

nature of the tautomers, being negative for **a** and positive for **h** in accordance with other reports on related dye series[43,44] and implying an inversion of the colour sequence.

HMO calculations on a variety of tautomeric dyes suggest that this kind of behaviour is the rule rather than the exception for $\mathrm{R{-}A\cdot N{=}N\cdot B{-}XH \rightleftharpoons R{-}A\cdot NH{-}N{=}B{=}X}$ type structures where A and B denote carbocyclic aromatic residues, XH is a protic donor and R is an inductive substituent in the sense discussed above. This point should be exemplified on phenylazonaphthols **2**. For the theoretical prediction of the sign of correlation we shall assume that the essential features of the dye chromogen are retained in the fragment **5**, which is justified by the close similarities of the relevant MOs and their energies in **2** and **5** (cf. Fig. 9). Moreover, **5** is also the smallest possible sub-unit that contains both potential protonation sites necessary for tautomeric discrimination. The R—Ph residue, rather than R alone, is then considered as an inductive substituent, altering the electronegativity of the nitrogen atom (N_β) to which it is attached. An electron acceptor R decreases the electronegativity of N_β and brings about a bathochromic shift of the transition if the π-density at this position increases upon excitation. Such a situation is encountered in the azo type fragment **5a** (cf. Fig. 11), thereby explaining the negative slope found for **1a** in Fig. 10a. In the hydrazone **5h**, on the other hand, a small π-density decrease at N_β accompanies the excitation, in agreement with the observed positive correlation for **4h** (Fig. 10b).

It follows from the above arguments that in azo structures a conjugating electron-withdrawing R and in the hydrazone tautomers a conjugating electron-donor substituent is needed to achieve the strongest bathochromic effect. This opposite spectral behaviour of the tautomers explains sufficiently the inversion of colour sequence.

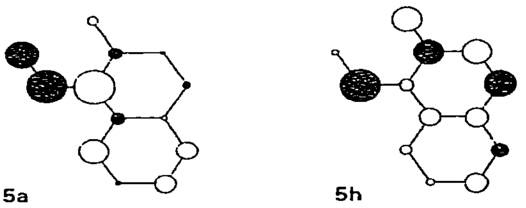

Fig. 11. Electron density difference maps of **5a** and **5h**. The area of the circles is proportional to $(c^2_{\mathrm{LUMO},i} - c^2_{\mathrm{HOMO},i})$. Shading represents an increase, empty symbols a decrease, of electron density upon excitation.

A further consequence concerns the hydrazones, the present domain of which includes colours from yellow to orange.[46] It should be possible to extend this range towards blue by the augmentation of electron donors in the diazo component provided the tautomeric equilibrium is kept fixed on the **h** side by some structural means. We intend to report on this topic in a future paper.

5. CONCLUSIONS

The major findings of this work are:

(i) All naphthylamines studied of general structure **1** and **3** are in the azo form on properly dyed PES and WO fibres or in the adsorbed state in KBr pellets.

(ii) This behaviour is similar to that found in solutions and predicted by perturbational molecular orbital theory.

(iii) The investigated naphthol dyes **2** and **4** exhibit a hydrazone predominance in the environments described above, with the exception of the *p*-MeO derivatives, which are composed of both tautomeric species in comparable concentrations. The hydrazone content of these is substrate-dependent and increases in the order PES < WO < KBr.

(iv) A substituent R renders the colour band of the azo tautomer R—A · N=N · B—XH more bathochromic with increasing electron-withdrawing character (as measured by Hammett σ_R) by virtue of its inductive effect, but shifts the long wavelength transition of the hydrazone R—A · NH—N=B=X progressively towards higher frequencies.

(v) As a consequence of (iv) a completely different colour sequence might result in closely related dyes such as **1** and **2** if R is varied.

(vi) The conjugative effect of the substituent always exerts a bathochromic effect on the colour band of both tautomers, the magnitude of which is not related to σ_R. This leads in many cases to unacceptable $\tilde{\nu}$–σ_R correlations with great data-point scatter.

ACKNOWLEDGEMENTS

The authors are very much indebted to Dr H. Ackerman for a gift of dyed wool samples. We further thank U. Bergamin for the technical assistance with UV and Raman spectra, R. Griesser for help in colorimetric computations and O. Heiber for the calorimetric measurements. Textile dyeings were organized by P. Dussy, and the reflectance measurements by Dr M. Ribeaud and Dr H. Stadelmann; this is gratefully acknowledged.

REFERENCES

1. J. Kelemen, *Dyes and Pigments*, **2**, 73 (1981).
2. J. Kelemen, S. Moss, H. Sauter and T. Winkler, *Dyes and Pigments*, **3**, 27 (1982).
3. J. Kelemen, G. Kormány and G. Rihs, *Dyes and Pigments*, **3**, 249 (1982).
4. M. J. S. Dewar and R. C. Dougherty, *The PMO theory of organic chemistry*. New York, Plenum Press (1975).
5. W. B. Smith, *J. Chem. Ed.*, **48**, 749 (1971).
6. H. C. Longuet-Higgins, *J. Chem. Phys.*, **18**, 265 (1950).
7. J. Elguero, C. Marzin, A. R. Katritzky and P. Linda, *The tautomerism of heterocycles*, *Adv. Heterocyclic Chem.*, Supplement 1. New York, Academic Press (1976).
8. G. O. Dudek and E. P. Dudek, *J. Am. Chem. Soc.*, **88**, 2407 (1966) and references cited therein.
9. For reviews see I. Ya. Bershtein and O. F. Ginzburg, *Russ. Chem. Rev.*, **41**, 97 (1972); R. A. Cox and E. Buncel, in *Chemistry of the hydrazo, azo and azoxy groups*, Part 2, Chapter 18, p. 775, ed. S. Oatai. London, Wiley (1975); E. Sawicki, *Photometric organic analysis*, p. 166. New York, Wiley–Interscience (1970).
10. G. Gabor, Y. Frei, D. Gegiou, M. Kaganowitch and E. Fischer, *Isr. J. Chem.*, **5**, 193 (1967).
11. V. Bekárek, K. Rothschein, P. Vetešnik and M. Večeřa, *Tetrahedron Lett.*, 3711 (1968).
12. V. Bekárek, J. Dobáš, J. Socha, P. Vetešnik and M. Večeřa, *Coll. Czech. Chem. Commun.*, **35**, 1406 (1970).
13. A. Lyčka, D. Šnobl, V. Machaček and M. Večeřa, *Org. Magn. Resonance*, **16**, (1981).
14. A. Lyčka and D. Šnobl, *Coll. Czech. Chem. Commun.*, **46**, 892 (1981).
15. R. Kuhn and F. Baer, *Ann.*, **516**, 143 (1935).
16. A. Burawoy, A. G. Salem and A. R. Thompson, *J. Chem. Soc.*, 4793 (1952).
17. A. H. Berrie, P. Hampson, S. W. Longworth and A. Mathias, *J. Chem. Soc.*, *Sect. B*, 1308 (1968).
18. D. Hadži, *J. Chem. Soc.*, 2143 (1956).
19. G. Kortuem, *Reflectance spectroscopy*, (a) p. 176, (b) p. 1, (c) p. 103. Berlin, Springer-Verlag (1969).
20. M. Kurahashi, *Bull. Chem. Soc. Japan*, **49**, 2927 (1976); *Chem. Lett.*, 181 (1974); M. Kurahashi, M. Fukuyo, A. Shimada and A. Kawase, *Bull. Chem. Soc. Japan*, **49**, 872 (1976); M. Kurahashi, A. Kawase, K. Hirotsu, M. Fukuyo and A. Shimada, *ibid.*, **45**, 1940 (1972).

21. I. Saito, Y. Bansho and A. Kakuta, *Kogyo Kagaku Zasshi*, **70**, 1715 (1967).
22. C. Dehari, Y. Matsunaga and K. Tani, *Bull. Chem. Soc. Japan*, **43**, 3404 (1970).
23. Y. Matsunaga and N. Miyajima, *Bull. Chem. Soc. Japan*, **44**, 361 (1971).
24. Y. Matsunaga and N. Miyajima, *Bull. Chem. Soc. Japan*, **45**, 3345 (1972).
25. R. Hempel and H. Viola, *Acta Polymerica*, **30**, 450 (1979).
26. R. Hempel, H. Viola, J. Morgenstern and R. Mayer, *J. Prakt. Chem.*, **318**, 983 (1976).
27. G. Wyszecki and W. B. Stiles, *Color science*, Sect. 3, p. 228. New York, Wiley (1976).
28. E. Schmidt, H. Loeliger and R. Zuercher, *Helv. Chim. Acta*, **61**, 488 (1978).
29. M. Davies and A. Edwards, *Trans. Faraday Soc.*, **63**, 2163 (1967).
30. T. Kobayashi, E. O. Degenkolb and P. Rentzepis, *J. Phys. Chem.*, **83**, 2431 (1979).
31. W. Reddish, *Trans. Faraday Soc.*, **46**, 459 (1950).
32. H. Rau, *Angew. Chem.*, **85**, 248 (1973).
33. G. Kortuem, J. Vogel and W. Braun, *Angew. Chem.*, **70**, 651 (1958).
34. C. H. Griffiths and A. R. Monahan, *Mol. Cryst. Liq. Cryst.*, **33**, 175 (1976).
35. A. R. Monahan and J. Kuder, *J. Org. Chem.*, **37**, 4182 (1972).
36. A. R. Monahan and J. B. Flannery, Jr, *Chem. Phys. Lett.*, **17**, 510 (1972).
37. J. H. Sharp and M. Lardon, *J. Phys. Chem.*, **72**, 3230 (1968).
38. F. W. Karasek and J. C. Decius, *J. Am. Chem. Soc.*, **74**, 4716 (1952).
39. P. A. Barrett, C. E. Deuland and R. P. Linstead, *J. Chem. Soc.*, 1719 (1936).
40. E. D. McRae and M. Kasha, in *Physical processes in radiation biology*, (eds. L. Augenstein, R. Mason and B. Rosenberg), p. 23. New York, Academic Press (1961).
41. H. Rau, *Ber. Bunsenges. physik. Chem.*, **72**, 637 (1968).
42. H. Rau, *Z. Naturforsch.*, **24b**, 494 (1969); *Ber. Bunsenges. physik. Chem.*, 73, 810 (1969).
43. J. Griffiths, *J. Soc. Dyers Colour*, **88**, 106 (1972).
44. E. Manda, *Bull. Chem. Soc. Japan*, **44**, 1620 (1971).
45. F. Gerson and E. Heilbronner, *Helv. Chim. Acta*, **42**, 1877 (1959).
46. J. Griffiths, *Rev. Prog. Coloration*, **11**, 37 (1981).
47. I. Bridgeman and A. T. Peters, *J. Soc. Dyers Colour.*, **86**, 519 (1970).
48. D. L. Ross and E. Reissner, *J. Org. Chem.*, **31**, 2571 (1966).
49. H. H. Jaafé, *Chem. Reviews*, **53**, 191 (1953).